



# Are the Italian microzonation level 2 abacuses applicable in the Friuli Venezia Giulia (Italy) plain? Comparison between the national abacuses and the numerically simulated amplification factors and between the derived elastic response spectra

Veronica Pazzi<sup>1</sup> · Chantal Beltrame ·  
Perla Taverna · Gabriele Peressi · Giovanni Costa<sup>2</sup>

Received: 7 November 2023 / Accepted: 22 March 2024  
© The Author(s) 2024

**Abstract** Seismic shaking of an area is strongly affected by the local geology. The so-called local site effects must be considered for the estimation of seismic effects on structures and urban planning. Thus, the seismic microzonation is the process aimed at identifying and mapping the subsoil local response in a given area, usually at urban/municipality scale and in terms of ground shaking parameters and susceptibility to ground instabilities. In Italy, for areas that can be schematised as a 1D

subsoil model (e.g. alluvial plain), a simplified approach is proposed to quantify the seismic amplification (amplification factor, AF). This approach consists of tables of correspondences, called seismic abacuses, available for the whole national area as well as for some regional territories, and derived for simplified subsoil models. In this work, the results of the comparison between the AF values retrieved from national abacuses applied in the Friuli Venezia Giulia (Italy) plain municipalities and those from 1D numerical simulations are presented. In general, the abacuses underestimate the local seismic site effects a part for sites with a shallow bedrock. No correlations/trends were identified between the AF derived from abacuses and those from numerical simulations. Moreover, considering the elastic acceleration response spectra, it emerges that in the 49.5% of the FVG analysed sites the abacuses approach, even though it underestimates the real seismic response, is a more suitable approximation compared to the soil class simplified approach proposed by the Italian regulation. Finally, what emerges is that the limit of 30 m, as indicated in the Italian regulation, to consider a deep or shallow bedrock seams underestimated, and the AFs are not correlated with the seismic bedrock depth when it is higher than 100 m.

## Highlights

- The microzonation level 2 national abacuses are not usable in Friuli Venezia Giulia Region (Italy).
- The national abacuses underestimate the seismic amplification in Friuli Venezia Giulia Region (Italy) plain.
- The plateau of elastic response spectra from abacuses and regulation simplified approach underestimate the real amplification.

V. Pazzi · C. Beltrame · G. Costa  
Department of Mathematics, Informatics and Geosciences,  
University of Trieste, Trieste, Italy

V. Pazzi (✉)  
Department of Earth Sciences, University of Firenze,  
Florence, Italy  
e-mail: veronica.pazzi@unifi.it

P. Taverna  
Center for Seismological Research, National Institute  
of Oceanography and Applied Geophysics, Udine, Italy

G. Peressi  
Civil Protection of the Friuli Venezia Giulia Region,  
Palmanova, UD, Italy

**Keywords** Seismic site effects · Local response ·  
Amplification factors · 1D seismic modelling ·  
Simplified approach · Elastic spectra form  
amplification factors

## 1 Introduction

A seismic hazard map expresses the spatial distribution of earthquake ground motion level/intensity (e.g. in terms of spectral acceleration—SA or peak ground acceleration—PGA) for a given exceedance probability (e.g. 10%) in a specific time interval (e.g. 50 years) at a specific site (McGuire 2008). In Europe, the up-to-date reference for seismic hazard studies is the 2020 European Seismic Hazard Model (ESHM20, <http://hazard.efehr.org/en/hazard-data-access/hazard-maps/>) that provides an update on the earthquake hazard assessment of the Euro-Mediterranean region (Danciu et al. 2021). In Italy, the up-to-date seismic hazard maps available at national scale (<https://esse1-gis.mi.ingv.it/>) have been released by Stucchi et al. (2011) and they are the current reference for seismic hazard studies. They provide PGA and/or SA values on rock sites for different exceedance probabilities in 50 years.

Local conditions (e.g. the geo-lithological stratigraphy, the presence of soft soils overlaying a rocky bedrock, and the depth of the water table) could affect the seismic shaking of an area and modify the seismic wave in terms of amplitude, frequency, and duration (Aki 1988; Forte et al. 2019; Kramer 1996). Subsoil nonplanar interfaces, in fact, generate surface waves that enhance the sediment amplification, extend the signal duration, and develop differential motions also interesting from an engineering point of view (Bard and Bouchon 1980a,b). According to the previous version of the Eurocode 8 (EN-1998 2004), five ground types (from A to E) characterised by a stratigraphic profile and given parameters (Table 3.1 of the Eurocode 8) can be identified and used in a simplified approach to account for the influence of local conditions on ground shaking. In case of uniform isotropic layer covering seismic (or engineering according to some authors, e.g. Falcone et al. 2021 and Mendicelli et al. 2022) bedrock (i.e. a layer characterised by a  $V_s \geq 800$  m/s that corresponds to the class A of the previous version of the Eurocode 8), the thickness of the cover layer and the shear wave velocity are the two factors that influence the amplification of a harmonic horizontal motion from the seismic bedrock to the surface. The Italian Building Code (NTC18 2018), and nowadays also the draft version of the Eurocode 8 revised in 2022, introduces the  $V_{sH}$  obtained by the same equation of the  $V_{s30}$  but

substituting 30 with H if  $H < 30$  m according to the following equation:

$$\begin{cases} V_{sH} = \frac{H}{\sum_{i=1,N} \frac{h_i}{V_{Si}}} H \in (0, 30\text{m}) \\ V_{s30} = \frac{30}{\sum_{i=1,N} \frac{h_i}{V_{Si}}} H > 30\text{m} \end{cases} \quad (1)$$

Thus, the equivalent/weighted average shear-wave velocity ( $V_{sH}$  or  $V_{seq}$  in this document) from the ground to the depth (H) of the seismic bedrock (if lower than 30 m) or from the ground to 30 m depth ( $V_{s30}$ , if the seismic bedrock is deeper than 30 m) is used in a simplified approach as a proxy for the seismic soil characteristics to design the appropriate site-dependent elastic response spectrum for structures (Castellaro and Mulargia 2009; EN-1998 2004; Forte et al. 2019; Mori et al. 2020, NTC18 2018).

However, real seismic wave propagation is more complex, so that the soil classes of the Eurocode 8 simplified approach could be not realistic. Seismic site/local response analysis is mandatory to characterise the soil behaviour, especially if the subsoil cannot be simplified as a 1D model, but 2D or 3D effects occur (Boaga et al. 2015; Forte et al. 2019; Lai et al. 2020; Mori et al. 2020; Peruzzi et al. 2016; Poggi et al. 2017). Accurate seismic site/local response analysis requires detailed knowledge of the subsurface, which is often not cost-effective if the number of sites is high. Thus, 1D seismic response simulation is still the main method to include site effects in engineering applications (Pilz and Cotton 2019).

The seismic microzonation (SM) is the process aimed at identifying and mapping, usually at urban/municipality scale and in terms of ground shaking parameters and susceptibility to ground instabilities, the subsoil local response in a given area. SM defines criteria and operational procedures to identify areas subjected either to geo-lithological ground amplification or ground instabilities (i.e. liquefaction, slope instability, and ground failures). Thus, SM is an essential tool for the local administrators in their anti-seismic urban planning, i.e. in developing strategies to reduce the level of damages in the most seismic hazardous areas and to deal with the critical situations caused by the occurrence of strong earthquakes (Crespellani 2014; Paolucci et al. 2020; Peruzzi et al. 2016). In Lai et al. (2020), there is a brief overview of the microzonation studies of the last 25 years.

In Italy, the Guidelines for Seismic Microzoning (Working Group ICMS 2008) have been standardised and published in 2008 (and subsequently updated after the 2009 L'Aquila earthquake) and have been in use since that date. These guidelines propose a modular approach that identifies three levels of details (Albarelo 2017; Lai et al. 2020; Moscatelli et al. 2020; Pagani et al. 2006; Paolucci et al. 2020; Peruzzi et al. 2016; Working Group ICMS 2008) based on the Manual for Zonation on Seismic Geotechnical Hazards (TC4 of ISSMGE 1999). The first level aims to build the reference subsoil geological model and identify and delimit areas (called micro-zones) with a homogeneous amplification behaviour with respect to the incoming seismic wave. Three main type behaviours (and thus areas) can be identified: (a) stable zones, i.e. areas that do not amplify the seismic wave, (b) stable zones prone to amplifications, i.e. areas subjected to geo-lithological and morphological ground amplification, and (c) zones prone to instability, i.e. areas that could be affected by seismic induced ground instabilities (i.e. liquefaction, active faults, and slopes). To do that, existing geologic, geomorphologic, geophysical, and hydrogeological data have to be collected and homogenised and new low-cost geophysical measurements can be carried out (Working Group ICMS 2008). The second and third levels aim at quantifying the seismic amplification of the different micro-zones (identified under the category (b) or (c) in the SM of level 1) with a homogenous behaviour in the seismic perspective and eventually re-shape these areas (Working Group ICMS 2008). In particular, seismic amplification is estimated by the computation of the amplification factor (AF), i.e. an integral spectral parameter defined as the ratio between the integrals in a period of time ( $T_1$  and  $T_2$ ) of the acceleration responses spectra of the output motion at the surface and of the input motion at the bedrock (Working Group ICMS 2008). The difference between the two levels rises in the approach. In the SM of level 2, a simplified approach called “seismic abacuses” (i.e. tables of correspondences which are also available for the whole national territory, Working Group ICMS 2008) is proposed for areas that can be schematised thanks to a 1D subsoil model (e.g. alluvial plain), where the presence of buried basins, that could induce 2D effects, or of shear velocity inversion can be excluded (as also discussed in “Abachi” Working Group 2015). The SM level 3 is based on numerical simulations to consider seismic phenomena strongly non-linear, to define actual

local seismic hazard, and to assess the local instability indexes (e.g. landslide index, liquefaction potential index, and consequent soil failures and subsidence values). This also implies that the elastic response spectra (NTC18 2018) can be obtained. Thus, additional non-invasive geophysical surveys are encouraged for SM of level 2, while are mandatory for SM of level 3 (Working Group ICMS 2008).

As underlined by Peruzzi et al. (2016), the abacuses should be representative of the specific litho/stratigraphical configuration of the study area, but they must be applicable over wide areas. Thus, they must be a balance between specialisation and generalisation. Given the nature of the ICMS national abacuses proposed by the Working Group ICMS (2008) and the limitations in their applicability highlighted by the ICMS working group itself, the development and use of regional ones is strongly recommended by the ICMS themselves. These regional abacuses should be developed considering the seismo-tectonic, the seismo-stratigraphic, and geologic peculiarities of the regional territories. Therefore, the national seismic abacuses may be used (a) as a term of comparison with the abacuses developed by the regions themselves; (b) temporarily, until specific ones have been prepared for their local context; and (c) definitively, after assessing the effectiveness to its local context (Sect. 1.6.3.2.2.1 of ICMS08). Examples of developed regional abacuses can be found in different regions of Italy, e.g. Tuscany (Peruzzi et al 2016), Emilia Romagna (Falcone et al. 2020a; Pagani et al. 2006; Tento et al. 2014), Latium (Pergalani et al. 2011), Lombardy (Pergalani and Compagnoni 2008), Abruzzo (Compagnoni et al. 2022), and Marche (Paolucci et al. 2020). In some cases, the structure of the ICMS “national” abacuses was followed more closely (e.g. for Lombardy region), while on other cases some significant changes were introduced (e.g. in the abacuses of Tuscany and Marche regions, where the sedimentary cover thickness ( $H$ ) was replaced by the fundamental frequency ( $f_0$ ) as proxy). Moreover, in the more recent abacuses (e.g. Paolucci et al 2020; Compagnoni et al. 2022), the AFs were defined for three different period intervals (0.1–0.5 s, 0.4–0.8 s, 0.7–1.1 s).

Until now, the assessment of the applicability of the national abacuses in the Friuli Venezia Giulia (FVG) Region was not carried out, nor regional abacuses were or will be developed, because the regional authorities in

charge of the SM decided to bypass the SM level 2 and directly support SM level 3 studies. Nevertheless, in the future for any reason, it would be possible that the local authorities will decide to fund SM level 2 studies. Thus, the main goals of this study were to assess the effectiveness of national abacuses to FVG local context and to prove and give evidences of the decision to bypass SM level 2, missing regional abacuses and not having at this time the intention to invest in developing them. Accordingly, in this work the results of the comparison between the AF values retrieved from national abacuses (AF,ab in the following) applied in the FVG plain municipalities and those from numerical simulations (AF,sim in the following) are presented. Moreover, as indicated in the ICMS08 (Working Group ICMS 2008) it is possible to use the AF,ab to reconstruct the surface elastic spectra starting from the elastic spectra for a class A soil (i.e. the spectrum referred to in the applicable legislation). Thus, in this work the procedure to reconstruct these spectra is presented, and the results are compared to those obtained from numerical simulations and from the soil class simplified approach.

Finally, in recent years Falcone et al. (2021) and Mendicelli et al. (2022) developed seismic AF national maps with different intervals of confidence and for different ranges of periods (0.1–0.5 s, 0.4–0.8 s, and 0.7–1.1 s, as required in the third level of the Italian microzonation). At the moment, in Italy, the estimation of the earthquake ground shaking maps is carried out considering, among the other things, the Vs30 national maps (e.g. Mori et al. 2020) as a proxy for the site effect (see Fornasari et al. 2022 and references therein). In the future, especially now that AF maps are available at national scale, this proxy could be changed. Thus, in this work the AF values obtained for the FVG plain by numerical simulation were compared to the Falcone et al. (2021) median AFs as a first attempt to evaluate the effectiveness of AF national scale maps.

A brief overview of the geology and seismicity of the FVG Region is shown in Sect. 2, while the procedure followed in this work is illustrated in Sect. 3. Results and discussion are proven in Sect. 4 and Sect. 5, respectively. Finally, in Sect. 6 some conclusions are presented.

## 2 Test site

The FVG Region is located in the north-east of Italy (insert in Fig. 1a) and corresponds to the

north-eastern portion of the Adria's microplate margin, where a complex interaction takes place between two orogenic chains: the Alpine chain in the northern part with an E–W trend and the Dinaric system in the eastern part with a NW–SE trend (Burrato et al. 2008; Mantovani et al. 1996; Slejko et al. 1989). The structural arrangement of the area is the result of the progressive convergence and rotation of the Adria microplate towards the Eurasian plate. This structure of South-Eastern Alps led to the generation of thrust and strike slip faults characterised in the past by destructive earthquakes with magnitudes between 5 and 7 (Burrato et al. 2008; Tiberi et al. 2014; Venturini et al. 2004). Analysing the distribution of the historical seismicity, it results that the events are mostly concentrated in the Prealps, whereas most faults are located in the mountain area. The main faults of the area, as retrieved by Tiberi et al. (2014), are shown in Fig. 1a and the linked historical earthquakes are listed in Table 1.

The FVG territory from a seismic hazard point of view, as visible from the seismic hazard map of the Euro-Mediterranean region ESHM20 (Danciu et al. 2021) shown in Fig. 1a, can be divided into two main areas. One is the mountain area in the northern part characterised by a moderate to high seismicity, and the other is the alluvial plain (the focus of this work) in the southern characterised by a low to moderate seismicity. Because FVG Region is a seismic area, there are several seismic monitoring networks. One of these is the FVG Accelerometric Network (RAF) which was installed in 1993 by the University of Trieste, with the cooperation of national and international institutes. It is part of the National Accelerometric Network (RAN) owned and managed by the Italian National Civil Protection (Costa et al. 2022). The RAF can be used both in monitoring and emergency whereas it transmits real time data to Civil Protection of Friuli Venezia Giulia, who can display and elaborate them immediately after an earthquake.

The study area (white rectangles in Fig. 1a and b) is the eastern portion of the wider Venetian–Friulian Plain that constitutes part of the foreland basin of the Southern Alps. This stretch of alluvial plain is characterised by alluvial megafans, i.e. very large fan-like features with a remarkable variety of texture between the apical and the distal portions (Fontana et al. 2008). According to Fontana et al. (2008) and Nicolich et al. (2004), the Plio-Quaternary deposits depth in the FVG plain is up



**Table 1** Location, data, and parameters of the main historical earthquakes from Burrato et al. (2008) and Tiberi et al. (2014). Events are listed from east to west. N/A stays for not available. The maximum macroseismic intensity (Imax) is expressed in MCS

Locality	Associated source	Associated earthquake(s)	Imax	Mw
Salò	N/A	Oct 31, 1901	N/A	5.7
Thiene	Thiene-Bassano	N/A	N/A	6.6
Asolano	Bassano–Cornuda	Feb 25, 1695	X	6.6
Montello	N/A	N/A	N/A	6.7
Cansiglio	Cansiglio	Oct 13, 1936	IX	5.9–6.1
Belluno	Polcenigo-Montereale	June 29, 1873	IX–X	6.3–6.4
Maniago	Maniago	July 10, 1776	VIII–IX	5.8–5.9
Tramonti	Tramonti	June 7, 1794	VII–VIII	5.6–5.8
Sequals	N/A	N/A	N/A	6.5
Gemona	Gemona South Gemona East	May 6, 1976 Sept 15, 1976	IX–X VIII–IX	6.4 5.9–6.1
Villach	N/A	Jan 25, 1348	IX–X	6.7–7.0
Bovec	Bovec-Krn	Apr 12, 1998	N/A	5.7–5.8
Medea	Medea	1279?	N/A	6.4
Idrija	Idrija	Mar 26, 1511	X	6.5–6.8

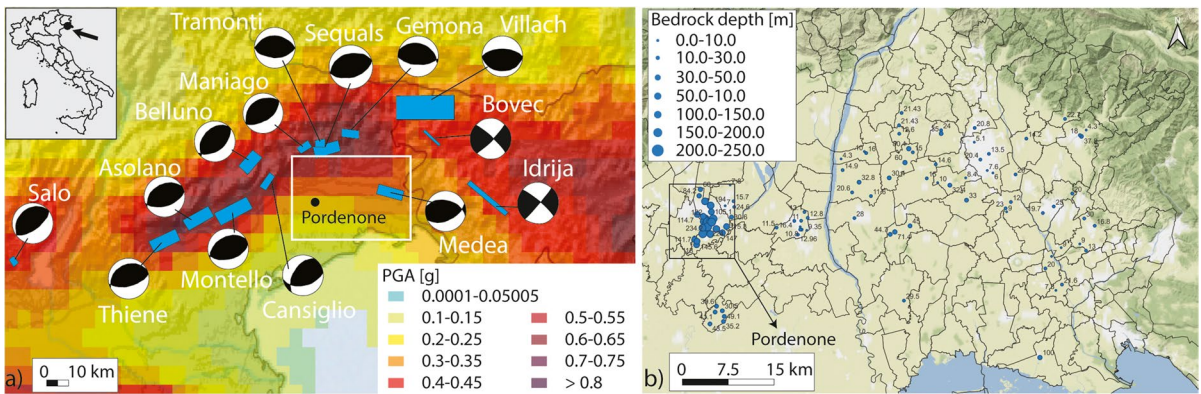


**Fig. 1** **a** Main faults (light blue rectangles) of the Alpine chain (northern part with an E–W trend) and of the Dinaric system (eastern part with a NW–SE trend) and related historical earthquakes (shown as their beachballs and listed in Table 1) as retrieved from Tiberi et al. (2014). The base map is the seismic hazard map of the Euro-Mediterranean region ESHM20 (Dan-

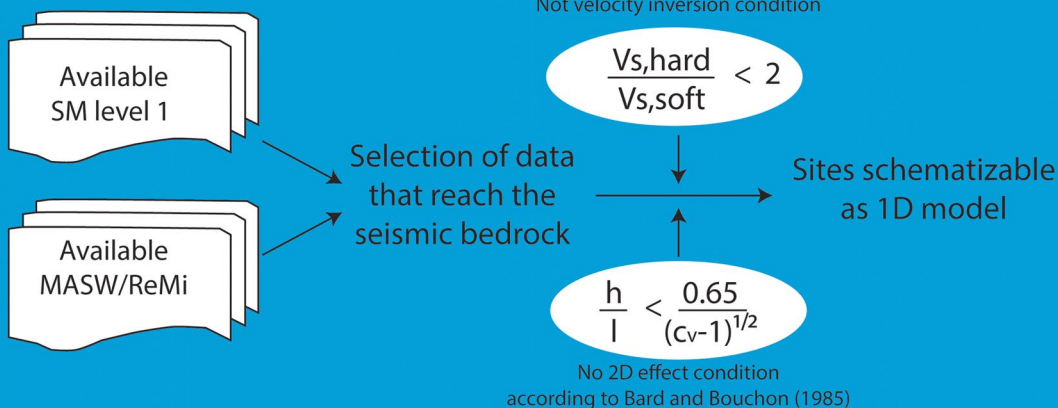
ciu et al. 2021). The white rectangle indicates the study area that is also shown in **b**. **b** Zoom on the study area showing the distribution of the analysed sites. The dimension of the blue dots is linked to the seismic bedrock depth as derived from boreholes and seismic surveys analysed in this study and collected from the SM level 1 as described in Sect. 3

to 1 km in the west portion and decrease up to 0.5 km in the east portion. This information has been confirmed by the analysis of the boreholes and seismic surveys collected for this study from the SM level 1 (and shown in Fig. 1b as blue dots). Consequently, the seismic bedrock depth increases from north to south and from east to west from few metres up to hundreds of metres in the Pordenone municipality (blue dots Fig. 1b), where the seismic bedrock depth is very high (up to 245.0 m) with a mean value of about 165.0 m.

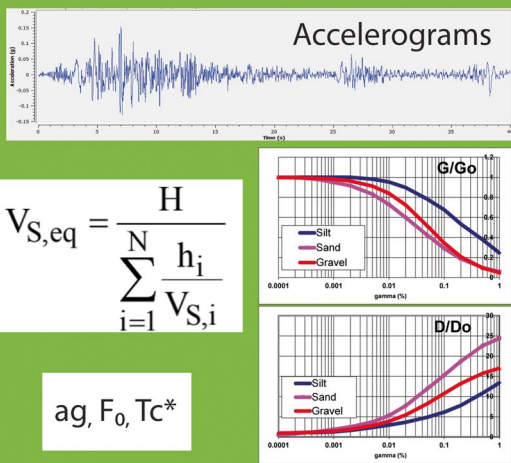
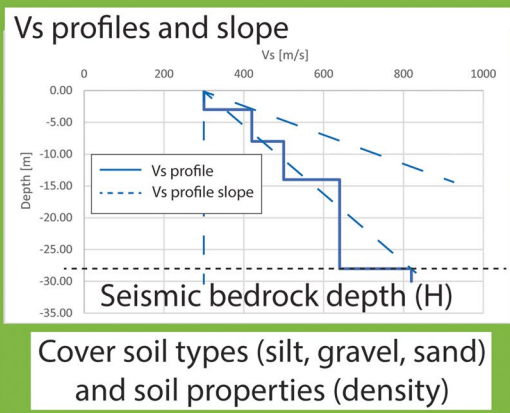
### 3 Material and methods

As in other works available in literature (e.g. Falcone et al. 2020a), the methodology proposed in this work consists in the comparison between the results from abacuses, simplified approaches, and specific analyses. The workflow followed in this work to compare (a) the AF,ab with the AF,sim and (b) the derived elastic acceleration response spectra is illustrated in Fig. 2. Four main steps can be identified in

### Preliminary phase



### Input selection phase



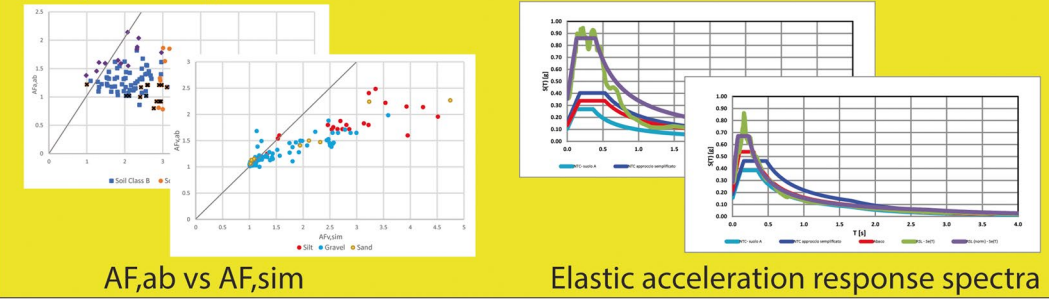
### AF calculation phase

Station	Amplification	Soil Class	$A_{Fa,ab}$	$A_{Fv,ab}$
1	1.2	Silt	1.5	1.8
2	1.5	Sand	1.8	2.2
3	1.8	Gravel	2.2	2.8
4	2.2	Silt	2.8	3.5
5	2.8	Sand	3.5	4.5
6	3.5	Gravel	4.5	5.5
7	4.5	Silt	5.5	6.5
8	5.5	Sand	6.5	7.5
9	6.5	Gravel	7.5	8.5
10	7.5	Silt	8.5	9.5
11	8.5	Sand	9.5	10.5
12	9.5	Gravel	10.5	11.5
13	10.5	Silt	11.5	12.5
14	11.5	Sand	12.5	13.5
15	12.5	Gravel	13.5	14.5
16	13.5	Silt	14.5	15.5
17	14.5	Sand	15.5	16.5
18	15.5	Gravel	16.5	17.5
19	16.5	Silt	17.5	18.5
20	17.5	Sand	18.5	19.5
21	18.5	Gravel	19.5	20.5
22	19.5	Silt	20.5	21.5
23	20.5	Sand	21.5	22.5
24	21.5	Gravel	22.5	23.5
25	22.5	Silt	23.5	24.5
26	23.5	Sand	24.5	25.5
27	24.5	Gravel	25.5	26.5
28	25.5	Silt	26.5	27.5
29	26.5	Sand	27.5	28.5
30	27.5	Gravel	28.5	29.5
31	28.5	Silt	29.5	30.5
32	29.5	Sand	30.5	31.5
33	30.5	Gravel	31.5	32.5
34	31.5	Silt	32.5	33.5
35	32.5	Sand	33.5	34.5
36	33.5	Gravel	34.5	35.5
37	34.5	Silt	35.5	36.5
38	35.5	Sand	36.5	37.5
39	36.5	Gravel	37.5	38.5
40	37.5	Silt	38.5	39.5
41	38.5	Sand	39.5	40.5
42	39.5	Gravel	40.5	41.5
43	40.5	Silt	41.5	42.5
44	41.5	Sand	42.5	43.5
45	42.5	Gravel	43.5	44.5
46	43.5	Silt	44.5	45.5
47	44.5	Sand	45.5	46.5
48	45.5	Gravel	46.5	47.5
49	46.5	Silt	47.5	48.5
50	47.5	Sand	48.5	49.5
51	48.5	Gravel	49.5	50.5
52	49.5	Silt	50.5	51.5
53	50.5	Sand	51.5	52.5
54	51.5	Gravel	52.5	53.5
55	52.5	Silt	53.5	54.5
56	53.5	Sand	54.5	55.5
57	54.5	Gravel	55.5	56.5
58	55.5	Silt	56.5	57.5
59	56.5	Sand	57.5	58.5
60	57.5	Gravel	58.5	59.5
61	58.5	Silt	59.5	60.5
62	59.5	Sand	60.5	61.5
63	60.5	Gravel	61.5	62.5
64	61.5	Silt	62.5	63.5
65	62.5	Sand	63.5	64.5
66	63.5	Gravel	64.5	65.5
67	64.5	Silt	65.5	66.5
68	65.5	Sand	66.5	67.5
69	66.5	Gravel	67.5	68.5
70	67.5	Silt	68.5	69.5
71	68.5	Sand	69.5	70.5
72	69.5	Gravel	70.5	71.5
73	70.5	Silt	71.5	72.5
74	71.5	Sand	72.5	73.5
75	72.5	Gravel	73.5	74.5
76	73.5	Silt	74.5	75.5
77	74.5	Sand	75.5	76.5
78	75.5	Gravel	76.5	77.5
79	76.5	Silt	77.5	78.5
80	77.5	Sand	78.5	79.5
81	78.5	Gravel	79.5	80.5
82	79.5	Silt	80.5	81.5
83	80.5	Sand	81.5	82.5
84	81.5	Gravel	82.5	83.5
85	82.5	Silt	83.5	84.5
86	83.5	Sand	84.5	85.5
87	84.5	Gravel	85.5	86.5
88	85.5	Silt	86.5	87.5
89	86.5	Sand	87.5	88.5
90	87.5	Gravel	88.5	89.5
91	88.5	Silt	89.5	90.5
92	89.5	Sand	90.5	91.5
93	90.5	Gravel	91.5	92.5
94	91.5	Silt	92.5	93.5
95	92.5	Sand	93.5	94.5
96	93.5	Gravel	94.5	95.5
97	94.5	Silt	95.5	96.5
98	95.5	Sand	96.5	97.5
99	96.5	Gravel	97.5	98.5
100	97.5	Silt	98.5	99.5

$A_{Fa,ab}$        $A_{Fv,ab}$



### Comparison phase



◀**Fig. 2** Flow chart followed to compare **a** the AF values retrieved from national abacuses (AF,ab) applied in the FVG plain municipalities and those from numerical simulations (AF,sim) and **b** the elastic acceleration response spectra obtained from 1D numerical analysis and abacuses. In the blue portion:  $V_s$  is the velocity of the shear waves,  $h$  is the depth of the valley,  $l$  is the valley half-length, and  $C_v$  is the ratio between the  $V_s$  of the seismic bedrock and the mean  $V_s$  of the soft layers. In the green portion:  $ag$ ,  $F_0$ , and  $T_c^*$  are the site parameters to build the target spectrum according to the Italian regulation (NTC18 2018)

the followed process: (1) a preliminary phase (highlighted in blue in Fig. 2), (2) the input selection phase (highlighted in green in Fig. 2), (3) the AFs calculation phase (highlighted in orange in Fig. 2), and finally (4) the comparison phase (highlighted in yellow in Fig. 2).

### 3.1 Preliminary phase

As mentioned in Sect. 1, the simplified approach of the SM level 2 can be applied if the subsoil can be schematised thanks to a 1D model. Thus, in the presence of buried basins, i.e. concave forms of the seismic basement with fillings made up of soft soils, 2D effects can play a dominant role and therefore make the estimates of the abacuses unrealistic. To evaluate the presence of this type of effect, and therefore the applicability of the abacuses, as a first approximation according to the Italian guidelines (“Abachi” Working Group 2015, Working Group ICMS 2008), it is possible to use the simplified approach proposed by Bard and Bouchon (1985). Moreover, according to the Working Group ICMS (2008) the ICMS national abacuses cannot be applied if there is a velocity inversion in the  $V_s$  profile, i.e. the ratio between the  $V_s$  of the harder layer and the  $V_s$  of the softer one is higher than 2. Therefore, the preliminary phase (highlighted in blue in Fig. 2) was carried out to individuate the FVG municipalities that satisfy both the above-mentioned conditions, and thus to identify areas where it was possible to apply national abacuses. At the date of September 2022, 190 over 224 municipalities have carried out a SM study of level 1. Among these, only 43 municipalities are located in the alluvial plains and have data about linear seismic surveys such as MASW (multi-channel analysis of surface waves: Baglari et al. 2018 and references therein, Foti et al. 2018) and ReMi (refraction microtremor: Mulargia and Castellaro 2013 and references therein). These

two types of non-invasive geophysical surveys, in fact, allow to gain information about the subsoil shear wave velocity profiles ( $V_s$ -depth curves) and the seismic bedrock depth, necessary to verify the Bard and Bouchon (1985) approach, to apply abacuses, and to perform 1D seismic response analysis. In total, 201 non-invasive geophysical linear surveys were analysed, and among these, only the 103, distributed over 28 municipalities that reached the seismic bedrock, were considered for further analyses. It is important to remark here that for some surveys the  $V_s$ -depth profile did not clearly identify the depth of a layer with  $V_s=800$  m/s (i.e. the seismic bedrock), but a layer with a lower  $V_s$  values and then a layer with a higher  $V_s$  value. In these cases, a linear increase of the  $V_s$  with depth was assumed and thus, for these sites the depth of the seismic bedrock (i.e. the depth at which the  $V_s=800$  m/s is reached) was obtained by a linear interpolation between the last two  $V_s$  values (one lower than 800 m/s and one higher).

### 3.2 Input selection phase

In the input selection phase (Fig. 2), all the parameters needed to calculate the AF,ab, the AF,sim, and to apply the NTC18 simplified approach were collected. Table 2 summarises which parameters were used for which methods and the sources of these parameters.

### 3.3 AF calculation phase

During the third procedure phase (Fig. 2), the AF values have been calculated by means of abacuses and the 1D seismic response.

#### 3.3.1 AF,ab calculation

The abacuses (an example is shown in Fig. 2 on the left of the portion highlighted in orange and in Table 3) allow to obtain two different AF,ab values defined as follows: the amplification factor  $AF_{a,ab}$  that corresponds to the low period amplification factor and is determined around the proper period for which there is the maximum acceleration response, and the amplification factor  $AF_{v,ab}$  that corresponds to the amplification factor over long periods for which the maximum pseudo-speed response is obtained (Working Group ICMS 2008). The ICMS AF,ab values represent the mean of the results obtained by the 1D equivalent

**Table 2** Parameters and their sources needed to calculate the AF values from national abacuses (AF,ab), the AF,sim from numerical simulations, and to apply the NTC18 simplified approach.  $ag$ ,  $F_0$ , and  $T_c^*$  are the site parameters to build the

target spectrum according to the Italian regulation (NTC18 2018).  $V_{seq}$  and  $V_{s30}$  are defined in Eq. 1.  $G/G_0$  and  $D/D_0$  are the share modules and dumping curves

Parameter	Source	Abacuses	ID seismic response analysis	NTC18 simplified approach
$ag$ , $F_0$ , $T_c^*$	NTC18	x (only the $ag$ value)		x
$V_{seq}$ or $V_{s30}$	MASW/ReMi	x		x
$V_s$ -depth profiles (i.e. layers thickness and seismic wave velocities)	MASW/ReMi		x	
Slope of the $V_s$ -depth profile	MASW/ReMi	x		
Bedrock depth	MASW/ReMi	x	x	x
Soil type of the cover layer (i.e. silt, sand, or gravel)	Boreholes and literature data	x		
Physical properties (i.e. materials densities)	Soil sample analysis and literature data		x	
$G/G_0$ and $D/D_0$ curves	Working Group ICMS 2008		x	
Accelerograms	SEISM-HOMe		x	

non-linear numerical simulations of seismic wave propagation carried out (a) on a horizontally stratified subsoil model (characterised by (i) a bedrock depth is in the range of 5–150 m, (ii) a the density

$\gamma = 18.00 \text{ kN/m}^3$ , and (iii) the  $V_{sH}$  is in the range of 150–700 m/s), overlaying a seismic bedrock half-space (characterised by (a) the density  $\gamma = 20.00 \text{ kN/m}^3$  and a  $V_s = 800 \text{ m/s}$  and (b) considering seven

**Table 3** Example of abacuses to obtain AFa values for sand soil with an intermediate slope of the  $V_s$ -depth curve and for a reference peak ground acceleration  $ag = 0.06 \text{ g}$

H [m]	$V_{sH}$ [m/s]									
	150	200	250	300	350	400	450	500	600	700
5	2.42	1.86	1.67	1.52	1.31	1.17	1.09	1.04	1.02	1.00
10	2.44	2.41	2.08	1.77	1.53	1.36	1.24	1.18	1.06	1.02
15	1.82	2.27	2.23	1.99	1.75	1.57	1.41	1.29	1.13	1.05
20	1.65	7.95	2.10	2.01	1.83	1.66	1.50	1.37	1.19	1.07
25	1.61	1.77	1.94	1.91	1.79	1.68	1.53	1.42	1.22	1.09
30	1.5	1.72	1.79	1.82	1.72	1.61	1.51	1.42	1.24	1.10
35	1.34	1.68	1.76	1.69	1.64	1.56	1.46	1.39	1.23	1.09
40	1.28	1.60	1.72	1.67	1.55	1.50	1.43	1.35	1.21	1.09
50	1.14	1.43	1.63	1.62	1.54	1.44	1.34	1.29	1.16	1.07
60	0.99	1.38	1.52	1.55	1.50	1.43	1.33	1.25	1.13	1.03
70	0.90	1.25	1.49	1.48	1.44	1.38	1.31	1.25	1.12	1.01
80	0.84	1.15	1.39	1.45	1.38	1.33	1.28	1.23	1.11	1.01
90	–	1.07	1.30	1.40	1.38	1.30	1.24	1.19	1.10	1.01
100	–	1.02	1.23	1.33	1.34	1.27	1.22	1.17	1.08	1.00
110	–	0.96	1.17	1.26	1.30	1.28	1.20	1.15	1.06	0.99
120	–	0.90	1.11	1.23	1.24	1.23	1.20	1.13	1.04	0.97
130	–	0.86	1.07	1.18	1.20	1.20	1.18	1.13	1.02	0.96
140	–	0.80	1.03	1.15	1.17	1.16	1.14	1.12	1.03	0.94
150	–	0.76	0.99	1.10	1.15	1.14	1.12	1.09	1.02	0.93



input accelerograms) (Working Group ICMS 2008). Three main lithologies of the sediment cover (i.e. silt that groups all the cohesive lithologies, and sand and gravel that group all the incoherent ones) were considered. The curves of decrease of the shear stiffness modulus ( $G/G_0$ ) and the curves of increase of the damping ( $D$ ) were derived from the literature (Working Group ICMS 2008) for the three different lithologies. Moreover, three different slopes of the  $V_s$ -depth curve (i.e. constant, maximum slope, and intermediate slope) were considered (Working Group ICMS 2008). Finally, the seven input accelerograms used for the simulation were artificial and spectra-compatible with average spectra derived from hazard studies and referred to for three different values of reference peak ground acceleration (i.e.  $ag = 0.06$  g,  $ag = 0.18$  g, and  $ag = 0.26$  g).

Thus, the  $AF_{ab}$  values were obtained from the mean acceleration ( $A$ ) and velocity ( $V$ ) elastic response spectra values around the maximum of the input (i) and output (o) spectra according to the following equations (Working Group ICMS 2008):

$$\left\{ \begin{aligned} AF_a &= \frac{\frac{1}{T_{Ao}} \int_{0.5T_{Ao}}^{1.5T_{Ao}} SA_o(T) dt}{\frac{1}{T_{Ai}} \int_{0.5T_{Ai}}^{1.5T_{Ai}} SA_i(T) dt} \\ AF_v &= \frac{\frac{1}{T_{Vo}} \int_{0.8T_{Vo}}^{1.2T_{Vo}} SV_o(T) dt}{\frac{1}{T_{Vi}} \int_{0.8T_{Vi}}^{1.2T_{Vi}} SV_i(T) dt} \end{aligned} \right. \quad (2)$$

Starting from the information collected as described in Sect. 3.2 and summarised in Table 2, the procedure to obtain  $AF_{ab}$  from the abacuses can be schematised as follows:

- (1) Individuate one of the three  $ag$  reference values ( $ag = 0.06$  g,  $ag = 0.18$  g, and  $ag = 0.26$  g): in this study, as also summarised in Table 2, the  $ag$  values of each site were obtained by interpolating the four nearest nodes of the  $ag$  grid provided by the NTC18 (2018) and, by approximation, the nearest reference  $ag$  value was selected.
- (2) Individuate the main lithology (i.e. silt, sand or gravel): in this study, it was retrieved from the boreholes available.
- (3) Individuate the slope of the  $V_s$ -depth curve (constant, maximum, or intermediate slope): the slope was assumed, according to the Working Group ICMS (2008), intermediate in most cases a part when the bedrock was shallow. To define

a numerical value of “shallow”, all the  $V_s$ -depth curves were plotted together and it was found that the slope could be considered maxima (i.e. characterised by a near-horizontal slope) when the bedrock was in the first 10 m.

- (4) Choose the abacus that corresponds to the individuated  $ag$ , lithology, and slope.
- (5) Choose the abacus row that corresponds to the seismic bedrock depth ( $H$ ): in this work, there were sites with a bedrock depth higher than the abacus maximum depth equal to 150 m. In that cases, the  $AF_{ab}$  for the last depth available were chosen also considering that recently Falcone et al. (2020b) demonstrated that the resonance frequency of soil sequences deeper than 100 m is lower than the resonance frequency of the wider diffused building types in Italy, and so sites with a bedrock depth higher than 100 m could be discharged from the analysis.
- (6) Choose the abacus column that corresponds to the site  $V_sH$ .
- (7) Individuate the  $AF_{ab}$  value that is located at the intersection between the row and the column selected at point 5 and 6, respectively (an example is shown in Fig. 2 by means of the black rectangles on the left of the portion highlighted in orange).

### 3.3.2 $AF_{sim}$ calculation

Following the procedure described by Working Group ICMS (2008) and the Order n. 55 of the April 24, 2018 of the Presidency of the Council of Ministers (<https://dev.sisma2016data.it/wp-content/uploads/2018/04/ordinanza-n.-55-delocalizzazioni-con-modifiche-approvate-ed-AEDES-con-allegato-24.04.18.pdf>), the amplification factors ( $AF_{sim}$ ) were calculated from the mean of the 1D-simulation outputs and the mean of the seven inputs (Mori et al. 2020; Paolucci et al. 2020) as the ratio between the integral of mean output response spectrum and the integral of mean input spectra. The integrals are computed around the maximum (i.e. the plateau) of both spectra. It implies that each maximum could refer to a different period range. The general  $AF$  equation is shown on right in the orange part of Fig. 2, where  $S_a(T)$  stays for the output mean spectrum and  $S_b(T)$  for the mean of the input one. Nevertheless, according to recent literature (Working

Group ICMS 2011; Paolucci et al. 2020; Falcone et al. 2021), it is more appropriate to calculate AF values as the ratio of the output and input response spectra integrals referred to the same period interval. Therefore, AF<sub>sim</sub> were also provided for different period ranges: AF0105 (0.1 s and 0.5 s), AF0408 (0.4 s and 0.8 s), and AF07115 (0.7 s and 1.1 s).

The 1D seismic response analysis has been performed by means of STRATA free software (Kottke et al 2009) that performs the numerical simulation applying a linear equivalent procedure to consider the non-linear soil behaviour. The software allows to model the site by means of continuous parallel plane layers overlaying a half-space corresponding to the seismic bedrock. Doing that, STRATA assumes that: (a) the stratigraphy is laterally homogeneous, isotropic, and infinite, and characterised by the linearised viscoelastic Kelvin-Voigt behaviour; (b) the stratified layers model the vertical heterogeneity, thus, each layer (i) is characterised by thickness ( $h_i$ ), shear wave velocity ( $V_{S,i}$ ), initial shear modulus ( $G_{0,i}$ ), and initial damping ratio ( $D_{0,i}$ ); (c) the seismic bedrock is considered deformable to take into account the loss of energy caused by the waves transmitted into the underlying rock and thus it is characterised by density ( $\gamma_{bedrock}$ ), shear wave velocity ( $V_{S,bedrock}$ ), and constant damping ratio ( $D_{bedrock}$ ). The seismic input is applied vertically at the interface between the half-space and the base of the stratified layers.

To accomplish this kind of analysis, as summarised in Table 2, the geo-lithological and geophysical parameters of the soil and the input accelerograms are needed. The  $h_i$ ,  $V_{S,i}$ , and  $V_{S,bedrock}$  values of each layer were obtained from the data available from the SM level 1; the densities ( $\gamma$ ) were obtained from literature and the following values were employed: 18.0 kN/m<sup>3</sup> for sand, 19.0 kN/m<sup>3</sup> for gravel, 20.0 kN/m<sup>3</sup> for silt, and 25 kN/m<sup>3</sup> for the seismic bedrock. The normalised share modulus curve (the  $G/G_0$  curve) and the damping model (the  $D/D_0$  curve) were retrieved from Working Group ICMS (2008). According to the Italian regulation, the accelerograms used to define the input to dynamic analyses in geotechnical and structural engineering have to be real time series recorded at outcropping rock sites with flat topographic conditions and in-the-mean spectrum-compatible to the acceleration response spectrum of the class A of the Italian Building Code (Bommer and Acevedo 2004; NTC18; Rota et al. 2012). Real accelerograms, in fact, compared to artificial or synthetic ones (allowed by the regulation for different kind

of analysis), are more realistic in relation to the seismogenic parameters and thus in terms of energy content, duration, frequency, number of cycles, and vertical-horizontal components correlation (Rota et al. 2012). Nevertheless, accelerograms are influenced by multiple sources of uncertainty so their selection is not unique. In literature, there are many selection procedures, e.g. Rexel (Iervolino et al. 2010) or the procedure developed by Genovese et al. (2019) or haseIREC (Zuccolo et al. 2021). In this work, seven accelerograms have been selected by means of the SEISM-HOME Web-GIS application (Rota et al. 2012) that provides, at any location of the national territory, the suite of seven seismic traces complying with the NTC18 (2018), i.e. accelerograms (a) real spectrum-compatible, (b) seismo-compatible, and (c) recorded at outcropping rock sites with flat topographic surface.

In the following, these notations will be used: AF<sub>a,ab</sub> and AF<sub>a,sim</sub> will indicate the AF<sub>a</sub> obtained by abacuses and seismic modelling, respectively, while AF<sub>v,ab</sub> and AF<sub>v,sim</sub> will indicate the AF<sub>v</sub> obtained by abacuses and seismic modelling, respectively.

### 3.4 Comparison phase

Finally, in the last phase (Fig. 2), the AF<sub>i,ab</sub> (where i stays for a and v) and the AF<sub>i,sim</sub> were compared and some useful lessons for the readers were obtained. The results are illustrated in the next section. Moreover, for each site four different elastic acceleration response spectra were generated and compared. They are (i) the 1D numerical simulation response spectrum (the output of the software); (ii) the one obtained regularising the previous spectrum according to the Italian regulation (NTC18 and Order n. 55 of the April 24, 2018 of the Presidency of the Council of Ministers, Working Group ICMS 2008); (iii) the elastic response spectra obtained by AF<sub>ab</sub> values; and (iv) the elastic response spectra for the site class deduced on the basis of the  $V_{seq}$  according to the NTC18 simplified approach.

The elastic response spectrum from AF<sub>ab</sub> values is drawn starting from the elastic response spectra for the site class A according to the following steps (Working Group ICMS 2008):

- (1) Calculate the spectral acceleration value ( $SA_C$ ) of the plateau of the spectrum for the site class A according to:  $SA_C = a_g * F_0$ .

- (2) Calculate the spectral acceleration value ( $SA(1s)$ ) at  $T=1$  s of the spectrum for the site class A.
- (3) Compute  $T_C$  according to  $T_C = (SA(1s) * AFv)/(SA_C * AFa)$ .
- (4) Compute  $T_B = T_C/3$ .
- (5) Compute  $T_D = 4 * a_g + 1.6$  according to the NTC18 (2018).
- (6) Draw the spectrum between  $T=0$  and  $T = T_B$  as linear with  $SA(0) = a_g * AFa$  and  $SA(T_B) = SA_C * AFa$ .
- (7) Draw the spectrum between  $T = T_B$  and  $T = T_C$  (the spectrum portion characterised by constant acceleration) as constant  $SA(T) = SA_C * AFa$ .
- (8) Draw the spectrum between  $T = T_C$  and  $T = T_D$  (the spectrum portion characterised by constant velocity) as  $SA(T) = SA_C * AFa * T_C/T$ .

#### 4 Results

In Fig. 3 and in Fig. 4, the relations between the AFa and AFv values, respectively, retrieved from abacuses (vertical axes, AF,ab) and from the 1D numerical simulation (horizontal axes, AF,sim), are shown in relation (a) to the soil category as deduced by the Italian regulation on the basis of the  $V_{seq}$  (NTC18 2018), (b) to the lithology of the cover soil, (c) to the slope of the  $V_s$ -depth curve (in this work assumed as maxima if the bedrock depth was in the first 10 m), and (d) to the seismic bedrock depth divided in three classes according to the definition of  $V_sH$  (a class with  $z < 30$  m that represents areas where the  $V_sH$  were calculated and considered, a class with  $30 \text{ m} < z < 150$  m represents areas where the  $V_{s30}$  were calculated and used, and a class with  $z > 150$  m that comprises areas outside the limits of the abacuses). The values of the Pearson correlation coefficient for each data subset are summarised in Table 4.

Among all the analysed sites, 62 belong to the soil class B, 29 to the soil class C, and 12 to the soil class E. In general, both the AFa and AFv values obtained through the seismic modelling are higher than those obtained from the abacuses. Moreover, some AFa,ab values are lower than 1 while all the AFa,sim are equal or higher than 1. As a first approximation, it is possible to observe that there is no correlation between simulated values and those obtained from abacuses. From Fig. 4a, it can be seen that for class

E sites the AFv values obtained from the abacuses (purple rhombi) are comparable with those obtained from modelling, while the greatest range of variations is for site of class C (orange rhombi), as in the case of the factor AFa (Fig. 3a). From a lithology point of view, silt soils have the highest AF,sim values (up to about 5 for AFa and up to about 4.5 for AFv), except for one isolated sand sites. Analysing the AF values in relation to the slope of the  $V_s$ -depth curve, it is possible to observe that AF,ab greater than AF,sim can be found only for those sites where the slope is maximum, i.e. in general, for those sites where the seismic bedrock is shallow. Apart from some isolated values, the AFa,sim ranges for sites characterised by a bedrock depth lower than 30 m, and higher than 30 m are 1 to 3 and 2 to 5, respectively, while the AFv,sim ranges are 1 to 2 and 1.25 to 4.5, respectively.

In Fig. 5, an example of the comparison among the obtained elastic response spectra is shown. In this figure, the elastic response spectra obtained applying abacuses AFs is shown in red, the one obtained smoothing the seismic response analysis output according to the Italian regulation (NTC18 2018; Working Group ICMS 2008) is shown in dashed dark green, and the seismic response (SR) analysis output is shown in green. Moreover, the elastic response spectra for the class A soil (NTC18 2018) and that for the site class, as deduced by the Italian Building Code simplified approach (i.e. on the basis of the  $V_{seq}$ ), are shown in light blue and blue, respectively. In 85 sites (that correspond to the 82.5% of the sites), the plateau of the seismic response spectra regularised according to the Italian regulation is the highest (Fig. 5a, b). In 51 of the 85 above-mentioned sites (i.e. in the 49.5% of the whole analysed sites, Fig. 5a), the plateau of the spectrum from abacus is higher than that obtained according to the regulation soil type simplified approach, while in 34 of the 85 sites (i.e. in the 33% of the whole dataset, Fig. 5b) is the contrary. The remaining 17.5% (Fig. 5c–f) is distributed as follows: in 8 sites (i.e. 7.8% of the whole dataset, Fig. 5c) the plateau of the elastic acceleration spectrum from abacus is higher than the numerical seismic response and the NTC simplified approach, while in 7 sites (i.e. 6.8% of the whole dataset, Fig. 5d) the plateau of the elastic acceleration spectrum from abacus is higher than the NTC simplified approach that is higher than the plateau of the numerical seismic response. Finally, in 2 sites (i.e. 1.9% of the whole dataset, Fig. 5e)

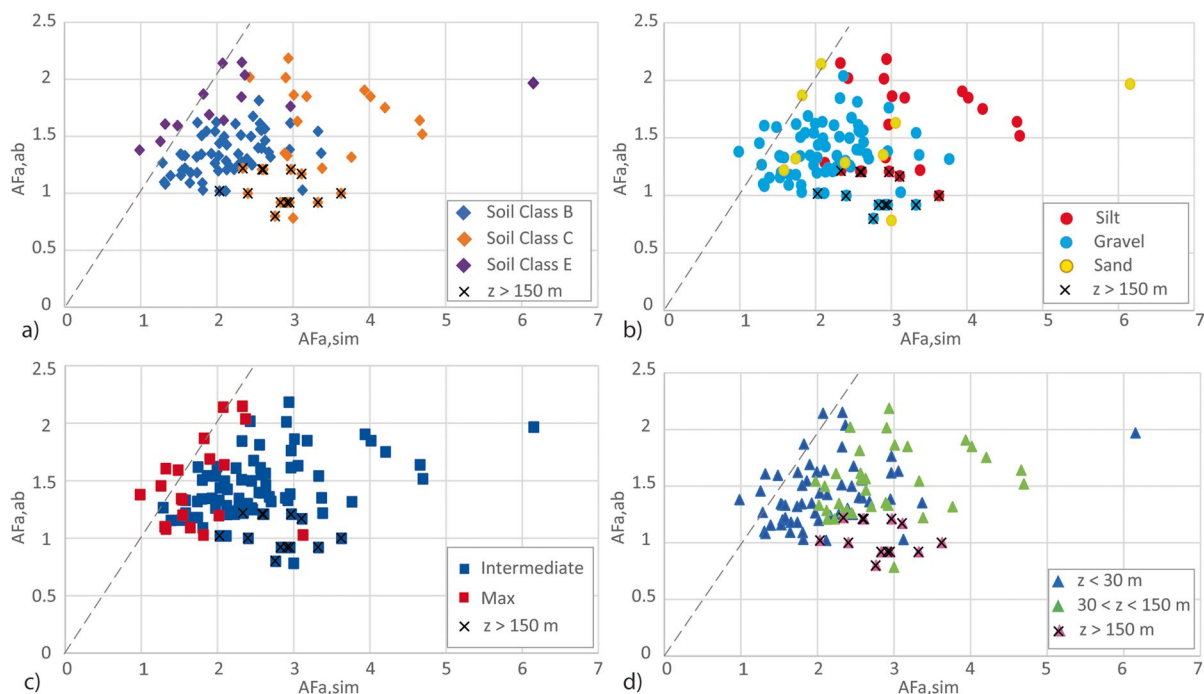


**Fig. 3** Comparison between the AFa values retrieved from abacuses (vertical axes) and from the 1D numerical simulation (horizontal axes) in relation to **a** the soil category as deduced by the Italian regulation on the basis of the Vseq (NTC18 2018), **b** the lithology of the cover soil, **c** the slope of the Vs-depth curve, and **d** the bedrock depth. In each panel,

the dashed line indicates the optimum condition, i.e. when AF,ab and AF,sim values are equal and data marked with a black x indicate those samples with a seismic bedrock higher than 150 m, and therefore, data for which the AF,ab is not well determined (see the text for a detailed explanation)

the plateau of the spectrum for the NTC simplified approach is higher than both the abacus and seismic response, and in 1 site (i.e. 1.0% of the whole dataset, Fig. 5f) the plateau of the spectrum for the NTC simplified approach is higher than the seismic response ones that is higher than the abacus one.

## 5 Discussion

The SM is a useful tool to classify the territory at local/municipality scale on the basis of the expected local seismic response. The aim of this study was to evaluate if the AF values retrieved for the SM of level 2 by national abacuses (i.e. the quantitative but simplified approach) are reasonable for the FVG plain and therefore applicable for the FVG plain, or if there is the need to develop regional abacuses.

Results (Figs. 3 and 4) show that the AF,sim values are in general higher than AF,ab. It means

that the abacuses underestimate the seismic site response. This assumption is not always true for those sites with a shallow bedrock and in soil class E (Figs. 3 and 4). It means that in the FVG plain where the seismic bedrock is shallow (up to 10 m) the national abacuses can overestimate the local AF. As already mentioned in Sect. 4, a correlation does not exist for the AF values. Figures 3 and 4 show that the AF values are clustered according to the soil class and type and to the depth of the seismic bedrock. In the 90% of the sites, in fact, the AFa,ab range span between 1 and 2, while AFa,sim between 1 and 5. In the same way, AFv,ab span between 1 and 3 while AFv,sim span between 1 and about 5. The AF,sim wider range was expected because the seismic response analysis better consider the local geo-lithological and geophysical variability of the site. On the contrary, the AF,ab underestimation was not expected because, being effective for the whole national territory, they were built in such a

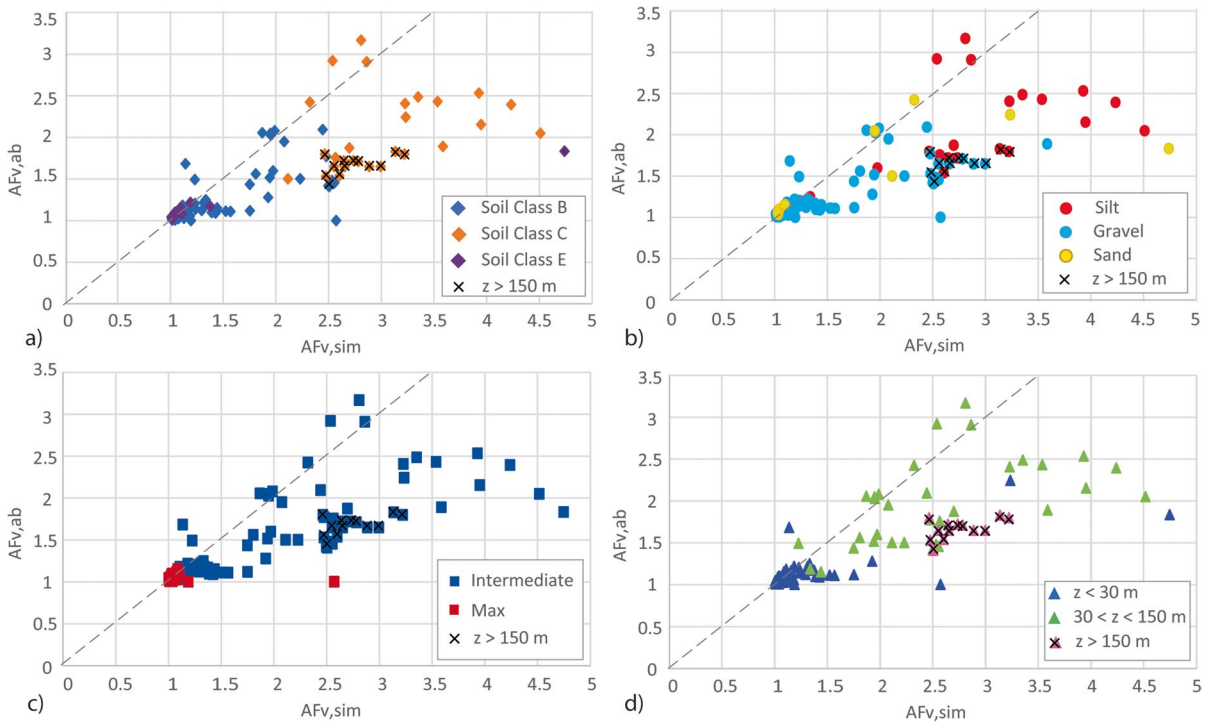


**Fig. 4** Comparison between the AFv values retrieved from abacuses (vertical axes) and from the 1D numerical simulation (horizontal axes) in relation to **a** the soil category as deduced by the Italian regulation on the basis of the Vseq (NTC18 2018), **b** the lithology of the cover soil, **c** the slope of the Vs-depth curve, and **d** the bedrock depth. In each panel,

the dashed line indicates the optimum condition, i.e. when AF<sub>v,ab</sub> and AF<sub>v,sim</sub> values are equal and data marked with a black x indicate those samples with a seismic bedrock higher than 150 m, and therefore, data for which the AF<sub>v,ab</sub> is not well determined (see the text for a detailed explanation)

**Table 4** Values of the Pearson correlation coefficient for each data subset (soil categories: B, C, and E; lithology: silt gravel, and sand; slope of the Vs-depth curve: intermediate and max-

ima; and seismic bedrock depth:  $z < 30$  m,  $30 < z < 150$  m, and  $z > 150$  m) in each subplot (from a to d) of Figs. 3 and 4

	AFa (Fig. 3)			AFv (Fig. 4)		
Soil category (subplot a)	Class B	Class C	Class E	Class B	Class C	Class E
	0.39	0.27	0.48	0.67	0.29	0.98
Lithology (subplot b)	Silt	Gravel	Sand	Silt	Gravel	Sand
	0.07	-0.01	0.26	0.53	0.74	0.68
Slope of the Vs-depth curve (subplot c)	Intermediate	Maxima	Intermediate	Maxima		
	0.30	0.25	0.75	-0.24		
Bedrock depth (subplot d)	$z < 30$ m	$30 < z < 150$ m	$z > 150$ m	$z < 30$ m	$30 < z < 150$ m	$z > 150$ m
	0.36	0.29	-0.23	0.73	0.57	0.56

way as to provide sufficiently conservative AF estimates (see Paolucci et al. 2020).

As already observed in Sect. 4, few AF<sub>a,ab</sub> values (6 over 103) are lower than 1 while all the AF<sub>a,sim</sub>

are higher than 1, and all the AFv values are always higher than 1. The sites with AF<sub>a,ab</sub> lower than 1 are all located in the Pordenone municipality: all the sites are in class C; in 5 sites the cover has been classified



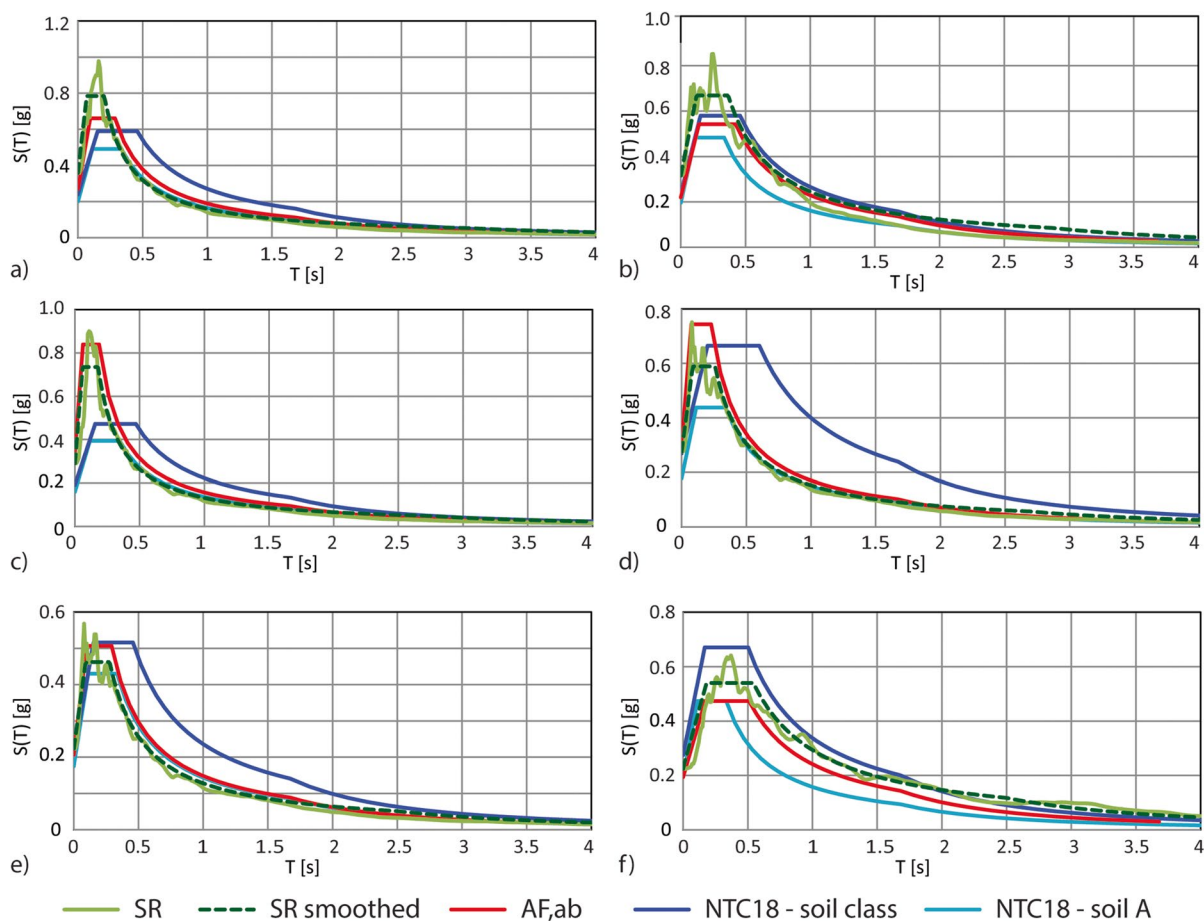


**Fig. 5** Examples of a comparison among the elastic response spectra: in all the panel in light blue the spectra for the class A soil (EN-1998 2004), in blue the one for the site class as deduced by the Italian Building Code simplified approach (i.e. on the basis of the  $V_{seq}$ ), in red the one obtained applying the abacuses AFs, in green the seismic response (SR) analysis out-

put, and in dashed dark green the seismic response analysis output smoothed according to the Italian regulation (NTC18 2018; Working Group ICMS 2008). **a** Flaibano sites, **b** Mereto di Tomba sites, **c** Casarla site, **d** Campofornido site, **e** Pavia di Udine site, **f** Pordenone site spectra

as gravel, and just 1 as sand. In 1 site, the bedrock depth is lower than 150 m and in the other cases it ranges between 150 and 245 m. It is important to remember that the abacuses are built for a maximum bedrock depth of 150 m, so in these last sites the abacuses are not really applicable. In both Figs. 3 and 4, these sites have been marked with a black “x” and seem to cluster in the lower part of the distribution.

According to the ICMS, the  $AF_{sim}$  were obtained according to Eq. 2: they are computed from the ratio between the integrals of output response and input response spectra computed around the maximum (i.e. the plateau) of both spectra. This implies that each maximum could refer to a different period range.

Thus, recently Falcone et al. (2021) and Paolucci et al. (2020) proposed to provide AFs for different period ranges (0.1–0.5 s, 0.4–0.8 s, and 0.7–1.1 s), so that the integrals of output and input response spectrum are referred to the same interval period. It is important to remember that the  $AF_a$  can be compared to the  $AF_{0105}$ , while the  $AF_v$  with  $AF_{0711}$ .  $AF_{0408}$  sometimes are comparable with  $AF_a$  and sometimes with  $AF_v$ . In Fig. 6, the  $AF_{a,sim}$  and  $AF_{v,sim}$  computed according to Eq. 2 as well as the AFs computed in the ranges 0.1–0.5 s ( $AF_{0105}$ ), 0.4–0.8 s ( $AF_{0408}$ ), and 0.7–1.1 s ( $AF_{0711}$ ) are shown in relation to the bedrock depth. It is possible to note that: (a) for the class E sites (in purple) the

AFa,sim increases with depth, while the AFv,sim is quite stable around 1 and consequently the AF0105 increases with depth, while the AF0408 and AF0711 are quite stable around 1. (b) For the class B sites (in blue), both AFa,sim and AFv,sim increase up to 50 m and then AFa,sim and AFv,sim range between 2 and 3 (apart some isolated cases) and between 1.5 and 2.5, respectively, while the AF0105 (dots) and AF0408 (triangles) values increase up to 50 m and then become stable between 1.5 and 3 (apart some isolated cases), and AF0711 (crosses) values are quite stable around 1 up to 40 m and then range between 2 and 3.5. (c) For class C sites (in orange), both the AFa,sim and AFv,sim increase up to a depth of 50 m as well as the AF0105, AF0408, and AF0711 values,

with values higher than class B and then, at a depth higher than 100 m they become quite stable in a range that span from 2 to 4. Thus, in Fig. 6 it is possible to note an increase of AF0105 values for all soil classes up to cover thickness of 40–50 m; moreover, an increase of AF0711 values is visible for thicker covers than 40–50 m, especially for soil class B. From these results, the limit of 30 m indicated in the regulation to consider the Vseq or the Vs30 as a proxy for the seismic soil characteristics to identify the appropriate site-dependent design spectrum for structures (Castellaro and Mulargia 2009; EN-1998 2004; Forte et al. 2019; Mori et al. 2020; NTC18 2018) seems slightly underestimated.

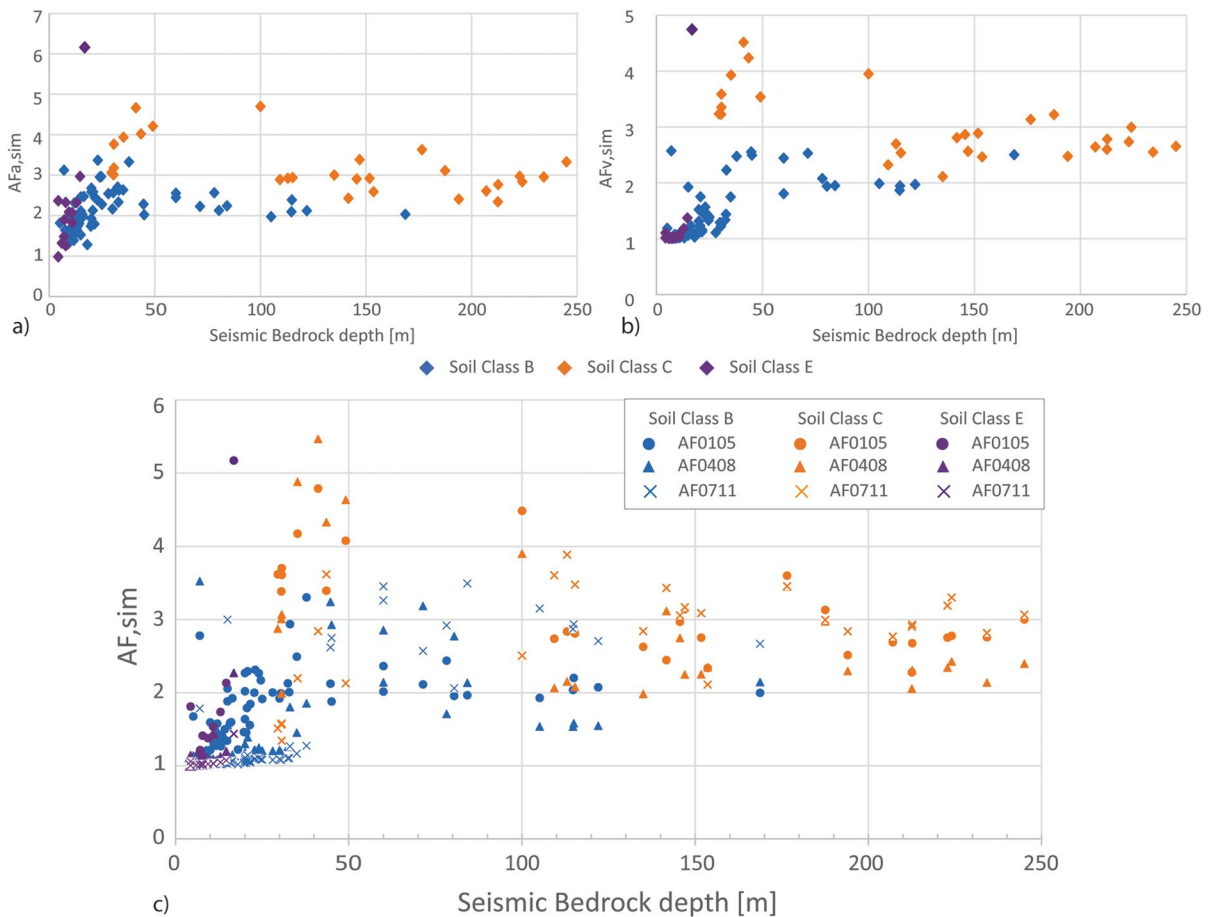


**Fig. 6** The AF,sim distribution in relation to the depth of the seismic bedrock. **a** The AFa,sim and **b** the AFv,sim computed according to Eq. 2. **c** The AF0105 (dots), AF0408 (triangles), and AF0711 (crosses) in relation to the soil categories (class B in blue, class C in orange, and class E in purple) computed

referring to the same period interval and provided for three different ranges (0.1–0.5 s, 0.4–0.8 s, and 0.7–1.1 s as in Falcone et al. 2021 and Paolucci et al. 2020). Please note that the three vertical axes have different scale ranges to better underline the variability of the values

The analysis and observation of the elastic acceleration spectra leads to two considerations: one about the time  $T_c$  (i.e. the corner period between the constant acceleration and constant velocity part of the elastic acceleration spectra), and one about the seismic local response smoothed spectra and its ability to effectively consider anomalous acceleration peak(s) in the local seismic response. It was observed that in most of the sites, the regulation simplified approach ( $T_c$ , NTC18—horizontal axis in Fig. 7a) overestimates the  $T_c$  time. This situation was found in sites of class E (pink stars in Fig. 7) and in most of the sites of the class C (yellow stars in Fig. 7), while for class B sites (blue stars in Fig. 7a) the difference between the  $T_c$  values is lower. This can be explained considering how the  $T_c$  value is calculated. From Fig. 7b, it emerges that in most of the sites the abacuses overestimate the  $T_c$  value and the overestimation is higher for sites in soil class C (orange dots in Fig. 7b).

It has been observed that the seismic response curves obtained by the numerical simulations are of two kinds. They are shown in Fig. 8. In Fig. 8a, the seismic response does not show significant peaks (type A in the following) while in Fig. 8b there is a peak higher than the others (type B in the following). Thus, the numerical simulation response output regularised to obtain design spectrum according to the Italian regulation (NTC18 2018; Working Group ICMS 2008), in case of seismic response of type A, better consider the real local seismic response. At the contrary, in case of seismic response of type B, the obtained elastic spectra underestimate the real soil

acceleration in the range of the frequency of the peak. This is a limit of the proposed approach. Site shown in Fig. 5d is the only example where the plateau of the spectrum from abacus is higher ( $AF_{a,ab} = 1.70$ ) than the plateau of the output of the simulation regularised to obtain design spectrum according to the Italian regulation ( $AF_{a,sim} = 1.54$ ). But, the abacus spectrum has values comparable with the maximum amplification of the output response spectrum. So, even for a wider range of periods, it can be considered reliable of the maxima amplification of the site. However, the plateau of the NTC18 response spectra underestimates the seismic response in more cases than the abacuses one. So, even if the abacuses underestimate the real seismic response, in 49.5% of the analysed sites they are more reliable than the NTC18 one.

As already indicated in Sect. 1, one limit of the national abacuses is their applicability only to stable areas susceptible to amplification and without 2D or 3D effects. Nevertheless, this work highlights some other general limitations in the applicability of the national abacuses. In particular, considering that the abacuses have been built for sites with a seismic bedrock between 5 and 150 m, results show that they could be not applicable in deep alluvial plains, because the  $AF_{a,ab}$  underestimates the local site effect. Moreover, from the results, it seems, at least for the FVG plain, that (a) the  $AF_{a,sim}$  values are not correlated with the seismic bedrock depth when it is higher than 100 m and (b) the limit of 30 m to consider the  $V_{seq}$  or the  $V_{s30}$ , as indicated in the Italian regulation, seems underestimated.

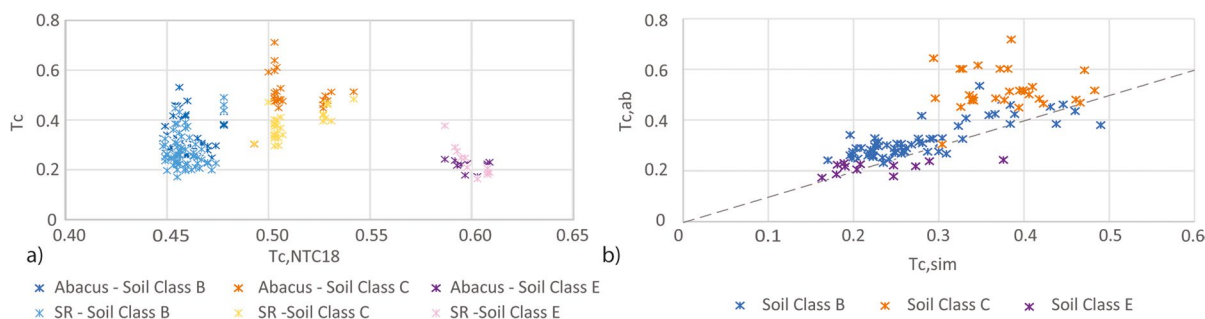


**Fig. 7** **a**  $T_c$  values (vertical axis) of the elastic response spectra obtained using the  $AF_{a,ab}$  values (dark colours) and the seismic response (SR) numerical analysis (light colours) shown in relation to the  $T_c$  values obtained by the Italian regulation for the soil category simplified approach (horizontal axis). Blue colours are for the soil class B sites, orange and yellow

for the soil class C sites, and pink and violet for the soil class E sites. **b**  $T_c$  values obtained by the seismic response numerical analysis ( $T_{c,sim}$ —horizontal axis) shown in relation to the  $T_c$  values obtained by the abacuses ( $T_{c,ab}$ —vertical axis). The dashed line indicates the optimum condition, i.e. when  $T_{c,ab}$  and  $T_{c,sim}$  values are equal.

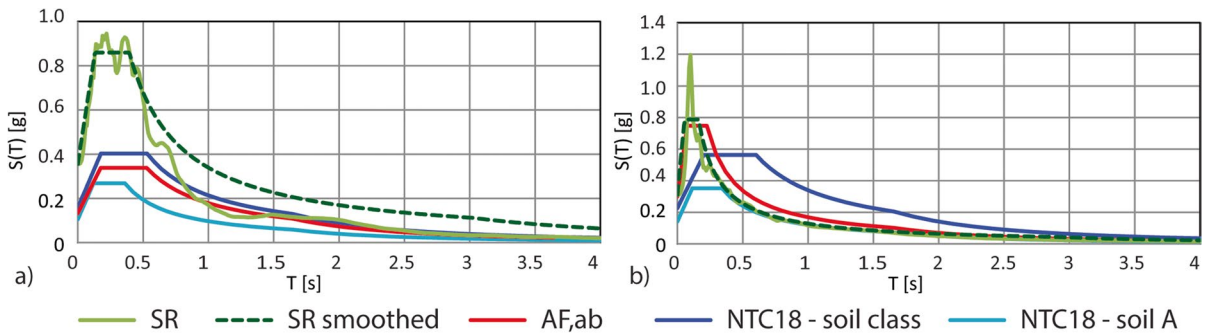


**Fig. 8** Elastic acceleration spectra for **a** a site where the seismic response spectrum from numerical simulations (light green line) does not shows significant peaks and **b** a site where

the seismic response spectrum from numerical simulations (light green line) shows a significant peak at a specific frequency

Another limitation in applying the abacus is linked to the selection of the main lithology of the cover layer. This limit occurs when it is not easy to deduce from the samples the dominant lithology, because the percentages of the three soil types (silt, sand, and gravel) are more or less the same or when a borehole in correspondence of the seismic line is missing. In this last case, also the numerical simulation of the local seismic site response could be affected by errors. In Fig. 9, is shown an example

for the Casarsa della Delizia municipality of how the AF,ab changes in relation to the chosen cover lithology. The AF,ab for sand soil cover is the highest, so it could be used as the most cautionary value.

As said in Sect. 1, in recent years the seismic amplification maps at national scale were calculated for different confidence intervals by Falcone et al. (2021) and Mendicelli et al. (2022) for three period intervals 0.1–0.5 s (AF0105), 0.4–0.8 s (AF0408), and 0.7–1.1 s (AF0711), as required in the third level

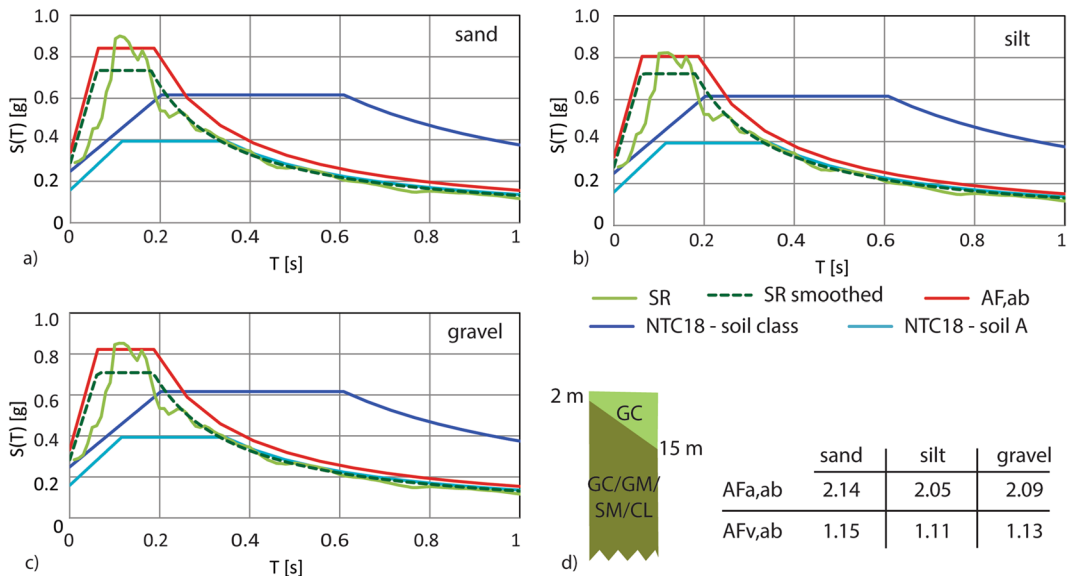


**Fig. 9** Example of how the cover soil lithology influences the seismic response (SR) and the AF,ab values (indicated in the table). In **a**, **b**, and **c** are shown the elastic spectra considering the cover soil as sand, silt, and gravel, respectively. In **d** is shown the subsoil stratigraphy as reported in the SM level 1

study: GC stays for clay gravel/gravel sand clay mixture; GM stays for silty gravel/gravel sand clay mixture and clay gravel; SM stays for silty sand/mixture of sand and silt; CL stays for inorganic clays of medium high plasticity/gravelly or sandy clays/silty clays

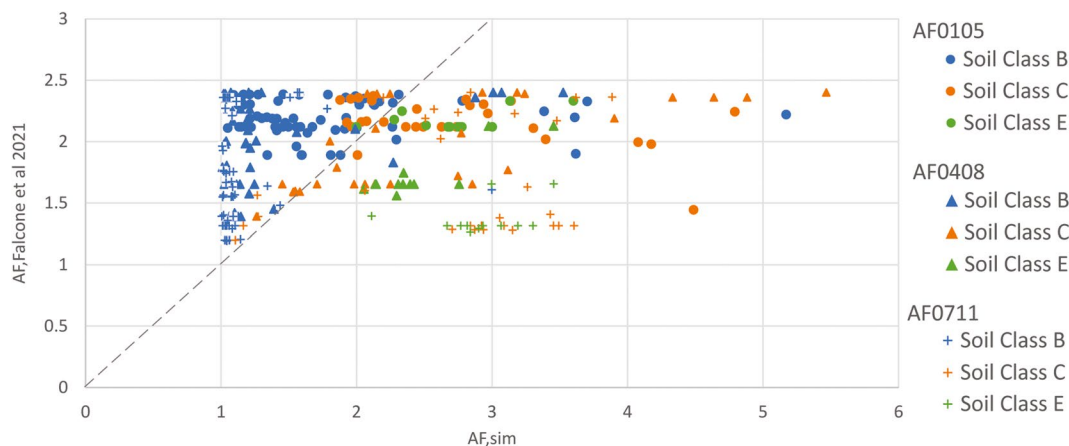


**Fig. 10** Comparison between the  $AF_{sim}$  and the median amplification factor  $AF$  by Falcone et al. (2021) for different period intervals (AF0105, AF0408, and AF0711). The dashed

line indicates the optimum condition, i.e. when  $AF_{sim}$  and  $AF$  by Falcone et al. (2021) values are equal

of the Italian microzonation. In the future, in Italy these maps could be employed in the generation of the earthquake shaking maps as a proxy for the site effects in place of the national  $Vs_{30}$  maps. Thus, as a first attempt to verify the reliability of the national  $AF$  maps, in Fig. 10 the comparison between the median amplification factor values obtained by Falcone et al. (2021) (vertical axis) and those obtained in this study (horizontal axis) is shown. It is possible to observe that all the values are higher than 1, confirming that the abacuses approach underestimates the seismic amplification of the FVG plain. Moreover, it is possible to observe that the  $AF_{Falcone}$  are limited in the range 1–2.5 (as also recently demonstrated by some works presented at the 2024 Italian National Congress of Geophysicist, the GNGTS, carried out in Ferrara from February 13th to 16th), while the range of  $AF_{sim}$  is wider (from 1 to 5.5). In general, the median  $AF_{Falcone}$  underestimates the soil class E amplification (green markers in Fig. 10) and, apart from some isolated cases for AF0408 and AF0711, underestimates the soil class C amplification (orange markers in Fig. 10). Most of the amplification factors of soil class B sites (blue markers in Fig. 10) are overestimated. To explain these differences, the simplifications carried out in the two different approaches have to be considered. From one side, in fact, to perform a study at national scale Falcone et al. (2021) adopted generated typical stratification columns and used the  $Vs_{30}$  calculated at national scale by Mori

et al. (2020). On the other side, in this study the stratification column obtained by boreholes and the  $Vs_{eq}$  gained from MASW and ReMi ad hoc surveys were used. Moreover, as also discussed earlier in this section, the 1D seismic numerical analyses sometimes show significant peaks at some frequencies. If the generated typical stratification columns are not able to reproduce these specific local conditions at those periods the AF0105, AF0408, and AF0711 from the two approaches will necessarily disagree.

## 6 Conclusion

This study was conducted to evaluate the reliability for the FVG alluvial plain municipalities of the Italian national abacuses proposed to carry out a SM of level 2. A limitation of this study relies on the  $Vs$ -depth profiles obtained by surface seismic measurements (no seismic boreholes data were available for the study area) that can affect by significant uncertainties the inversion procedure because of the non-uniqueness of the solution. Nevertheless, in general,  $AF$ s from abacus ( $AF_{ab}$ ) are lower than those obtained by means of 1D numerical simulations ( $AF_{sim}$ ), so the abacuses underestimate the local seismic response, demonstrating that the national ICMS abacuses do not satisfy the requirement that, as a simplified approach, they are “difficult” to be exceeded. Exceptions are some sites where the seismic bedrock is



shallow and the  $V_s$  reaches high values in few metres. In these sites,  $AF_{ab}$  overestimates the local seismic amplification. No correlations/trends were identified between the  $AF_{ab}$  and the  $AF_{sim}$ , but a clear cluster distribution occurs considering soil class (class B, C, and E in the 103 analysed sites), the soil type of the cover layer (silt, sand, and gravel), and the depth of the bedrock. The limit of 30 m to consider the  $V_{seq}$  or the  $V_{s30}$ , as indicated in the Italian regulation, seams underestimated, and the  $AF_{sim}$  values are not correlated with the seismic bedrock depth when it is higher than 100 m. Moreover, considering the response spectra, it emerges that in the 49.5% of the FVG analysed sites the abacuses approach, even though it underestimates the real seismic response, it is a more suitable approximation compared to the soil class simplified approach proposed by the Italian regulation that results in an excessive level of protection for a wider range of periods. The comparison with the median  $AF$  values, obtained by a study carried out at national scale to get reliable seismic amplification maps of Italy, is a first wake-up alarm on how local effects can be underestimated when the scale of the study is higher than a regional one. In conclusion, this study proves and gives evidences of the decision of the regional authorities in charge of the SM of directly support SM level 3 studies and bypass the application of ICMS abacuses. If, for any reason, the Friuli Venezia Giulia authorities in charge of the microzonation decide to rethink the applicability of SM level 2 studies for the municipalities of the region, this work provide evidences that it will be first of all necessary to develop regional abacuses.

**Acknowledgements** The results presented in this work have been achieved during the master thesis work of Beltrame Chantal and Taverna Perla. Authors want to thank Prof. Fabio Romanelli for the constructive discussions and Dr. Gaetano Falcone and his staff for providing the numerical values of their seismic amplification maps. The authors would also like to thank the editor and the reviewers for their useful comments which allowed them to improve the content of the work.

**Author contribution** Veronica Pazzi: conceptualisation, methodology, formal analysis, validation, writing—original draft, writing—review and editing, visualisation, supervision. Perla Taverna: conceptualisation, methodology, data curation, formal analysis, validation. Chantal Beltrame: conceptualisation, methodology, data curation, formal analysis, validation. Gabriele Peressi: conceptualisation, methodology, validation, supervision. Giovanni Costa: conceptualisation, methodology, validation, supervision. All authors commented on the original

versions of the manuscript. All authors read and approved the final manuscript.

**Funding** Open access funding provided by Università degli Studi di Firenze within the CRUI-CARE Agreement.

**Data availability** The datasets generated during and/or analysed during the current study are available from the corresponding author on reasonable request.

## Declarations

**Competing interests** The authors have no relevant financial or non-financial interests to disclose.

**Open Access** This article is licensed under a Creative Commons Attribution 4.0 International License, which permits use, sharing, adaptation, distribution and reproduction in any medium or format, as long as you give appropriate credit to the original author(s) and the source, provide a link to the Creative Commons licence, and indicate if changes were made. The images or other third party material in this article are included in the article's Creative Commons licence, unless indicated otherwise in a credit line to the material. If material is not included in the article's Creative Commons licence and your intended use is not permitted by statutory regulation or exceeds the permitted use, you will need to obtain permission directly from the copyright holder. To view a copy of this licence, visit <http://creativecommons.org/licenses/by/4.0/>.

## References

- “Abachi” Working Group (2015) Applicabilità degli abachi per la microzonazione sismica di livello 2. Proceedings of 34<sup>o</sup> Convegno Nazionale NGTTS, Trieste 17–19 novembre 2015, 109–113, (in Italian)
- Aki K (1988) Local site effects on strong ground motion. In: Earthquake engineering and soil dynamics II - recent advances in ground motion evaluation. June 27e30, Park City, Utah
- Albarelo D (2017) Extensive application of seismic microzoning in Italy: methodological approaches and socio-political implications. *Bollettino Di Geofisica Teorica e Applicata* 58(4):253–264. <https://doi.org/10.4430/bgta0205>
- Baglari D, Dey A, Taipodia J (2018) A state-of-the-art review of passive MASW survey for subsurface profiling. *Innov Infrastruct Solut* 3:1–13. <https://doi.org/10.1007/s41062-018-0171-2>
- Bard PY, Bouchon M (1980a) The seismic response of sediment-filled valleys. Part I The Case of Incident SH Waves. *Bull Seismol Soc Am* 70:1263–1286
- Bard PY, Bouchon M (1980) The seismic response of sediment-filled valleys. Part II. The case of incident P and SV waves. *Bull Seismol Soc Am* 70:1921–1941
- Bard PY, Bouchon M (1985) The two-dimensional resonance of sediment-filled valleys. *Bull Seismol Soc Am* 75(2):519–541

- Boaga J, Renzi S, Deiana R, Cassiani G (2015) Soil damping influence on seismic ground response: a parametric analysis for weak to moderate ground motion. *Soil Dyn Earthq Eng* 79:71–79. <https://doi.org/10.1016/j.soildyn.2015.09.002>
- Bommer JJ, Acevedo AB (2004) The use of real earthquake accelerograms as input to dynamic analysis. *J Earthquake Eng 8(spec01)*:43–91
- Burrato P, Poli ME, Vannoli P, Zanferrari A, Basili R, Galadini F (2008) Sources of Mw 5+ earthquakes in northeastern Italy and western Slovenia: an updated view based on geological and seismological evidence. *Tectonophysics* 453(1–4):157–176. <https://doi.org/10.1016/j.tecto.2007.07.009>
- Castellaro S, Mulargia F (2009) VS 30 estimates using constrained H/V measurements. *Bull Seismol Soc Am* 99(2A):761–773. <https://doi.org/10.1785/0120080179>
- Compagnoni M, Pergalani F, Basi M, Boncio P, Catenacci G, Durante F, Francescone M, Pace B, Pipponzi G, Pizzi A, Tallini M, Urbani A, Valentini A (2022) Construction of a level 2 microzonation abacus to evaluate local amplifications for the peri-Adriatic area in the Abruzzo region (Italy). *Bull Geophys Oceanogr* 63(4):597–618. <https://doi.org/10.4430/bgo00399>
- Costa G, Brondi P, Cataldi L, Cirilli S, Ertuncay D, Falconer P, Filippi L, Fornasari SF, Pazzi V, Turpaud P (2022) Near-real-time strong motion acquisition at national scale and automatic analysis. *Sensors* 22(15):5699. <https://doi.org/10.3390/s22155699>
- Crespallani T (2014) Seismic microzonation in Italy: a brief history and recent experiences. *Ingegneria Sismica* 21(2):3–31
- Danciu L, Nandan S, Reyes C, Basili R, Weatherill G, Beauval C, Rovida A, Vilanova S, Sesetyan K, Bard PY, Cotton F, Wiemer S, Giardini D (2021). The 2020 update of the European seismic hazard model: model overview. EFEHR technical report 001, v1.0.0. doi: <https://doi.org/10.12686/a15>
- EN-1998 (2004) Eurocode 8: design of structures for earthquake resistance—part 1: general rules, seismic actions and rules for buildings. Authority: the European Union per regulations 305/2011, Directive 98/34/EC, Directive 2004/18/EC, 1st ed. BSI, Brussels
- Falcone G, Acunzo G, Mendicelli A, Mori F, Naso G, Peronace E, Porchia A, Romagnoli G, Tarquini E, Moscatelli M (2021) Seismic amplification maps of Italy based on site-specific microzonation dataset and one-dimensional numerical approach. *Eng Geol* 289:106170. <https://doi.org/10.1016/j.enggeo.2021.106170>
- Falcone G, Boldini D, Martelli L, Amorosi A (2020a) Quantifying local seismic amplification from regional charts and site-specific numerical analyses: a case study. *Bull Earthq Eng* 18:77–107. <https://doi.org/10.1007/s10518-019-00719-9>
- Falcone G, Romagnoli G, Naso G, Mori F, Peronace E, Moscatelli M (2020) Effect of bedrock stiffness and thickness on numerical simulation of seismic site response Italian case studies. *Soil Dyn Earthq Eng* 139:106361. <https://doi.org/10.1016/j.soildyn.2020.106361>
- Fontana A, Mozzi P, Bondesan A (2008) Alluvial megafans in the Venetian-Friulian Plain (north-eastern Italy): evidence of sedimentary and erosive phases during Late Pleistocene and Holocene. *Quatern Int* 189(1):71–90. <https://doi.org/10.1016/j.quaint.2007.08.044>
- Fornasari SF, Pazzi V, Costa G (2022) A machine-learning approach for the reconstruction of ground-shaking fields in real time. *Bull Seismol Soc Am* 112(5):2642–2652. <https://doi.org/10.1785/0120220034>
- Forté G, Chioccarelli E, De Falco M, Cito P, Santo A, Iervolino I (2019) Seismic soil classification of Italy based on surface geology and shear-wave velocity measurements. *Soil Dyn Earthq Eng* 122:79–93. <https://doi.org/10.1016/j.soildyn.2019.04.002>
- Foti S, Hollender F, Garofalo F, Albarello D, Asten M, Bard PY, Comina C, Cornou C, Cox B, Di Giulio G, Forbriger T, Hayashi K, Lunedei E, Martin A, Mercierat D, Ohrnberger M, Poggi V, Renalier F, Sicilia D, Socco V (2018) Guidelines for the good practice of surface wave analysis: a product of the InterPACIFIC project. *Bull Earthq Eng* 16:2367–2420. <https://doi.org/10.1007/s10518-017-0206-7>
- Genovese F, Aliberti D, Biondi G, Cascone E (2019) A procedure for the selection of input ground motion for 1D seismic response analysis. In *Earthquake geotechnical engineering for protection and development of environment and constructions* (pp. 2591–2598) CRC Press
- Iervolino I, Galasso C, Cosenza E (2010) REXEL: computer aided record selection for code-based seismic structural analysis. *Bull Earthq Eng* 8:339–362. <https://doi.org/10.1007/s10518-009-9146-1>
- Kramer SL (1996) *Geotechnical earthquake engineering*. Prentice-Hall Inc., Upper Saddle River, New Jersey, p 7458
- Kottke AR, Wang XY, Rathje EM (2009) *Technical manual for Strata*. Pacific Earthquake Engineering Research Center, Berkeley, California, p 103
- Lai CG, Poggi V, Famà A, Zuccolo E, Bozzoni F, Meisina C, Bonì R, Martelli L, Massa M, Mascandola C, Petronio L, Affatato A, Baradello L, Castaldini D, Cosentini RM (2020) An inter-disciplinary and multi-scale approach to assess the spatial variability of ground motion for seismic microzonation: the case study of Cavezzo municipality in Northern Italy. *Eng Geol* 274:105722. <https://doi.org/10.1016/j.enggeo.2020.105722>
- Nicolich R, Della Vedova B, Giustiniani M, Fantoni R (2004) *Carta del Sottosuolo della Pianura Friulana* (Map of subsurface structures of the Friuli Plain). Progetto della Regione Autonoma Friuli Venezia Giulia, Direzione Centrale Ambiente e Lavori Pubblici (In Italian)
- NTC18 (2018) Ministero delle Infrastrutture e dei Trasporti. Decreto 17 gennaio 2018: Aggiornamento delle “Norme tecniche per le costruzioni”, *Gazzetta Ufficiale della Repubblica Italiana*, n. 42, 20 febbraio, Suppl. Ordinario n. 8. (in Italian) (available at: <https://www.gazzettaufficiale.it/eli/gu/2018/02/20/42/so/8/sg/pdf> last access March 14th, 2024).
- Mantovani E, Albarello D, Tamburelli C, Babbucci D (1996) Evolution of the Tyrrhenian basin and surrounding regions as a result of the Africa-Eurasia convergence. *J Geodyn* 21(1):35–72
- McGuire RK (2008) Probabilistic seismic hazard analysis: early history. *Earthq Eng Struct Dynam* 37(3):329–338. <https://doi.org/10.1002/eqe.765>

- Mendicelli A, Falcone G, Acunzo G, Mori F, Naso G, Peronace E, Porchia A, Romagnoli G, Moscatelli M (2022) Italian seismic amplification factors for peak ground acceleration and peak ground velocity. *J Maps* 18(2):497–507. <https://doi.org/10.1080/17445647.2022.2101947>
- Mori F, Mendicelli A, Moscatelli M, Romagnoli G, Peronace E, Naso G (2020) A new  $V_s30$  map for Italy based on the seismic microzonation dataset. *Eng Geol* 275:105745. <https://doi.org/10.1016/j.enggeo.2020.105745>
- Moscatelli M, Albarello D, Scarascia MG, Dolce M (2020) The Italian approach to seismic microzonation. *Bull Earthq Eng* 18(12):5425–5440. <https://doi.org/10.1007/s10518-020-00856-6>
- Mulargia F, Castellaro S (2013) A seismic passive imaging step beyond SPAC and ReMi. *Geophysics* 78(5):KS63–7KS2. <https://doi.org/10.1190/GEO2012-0405.1>
- Pagani M, Marcellini A, Crespellani T, Martelli L, Tento A, Daminelli R (2006) Seismic microzonation regulations of the Emilia-Romagna Region (Italy). Proceedings of Third International Symposium on the Effects of Surface Geology on Seismic Motion, Grenoble, France, 30 August 1 September 2006
- Paolucci E, Tanzini A, Peruzzi G, Albarello D, Tiberi P (2020) Empirical testing of a simplified approach for the estimation of 1D litho-stratigraphical amplification factor. *Bull Earthq Eng* 18:1285–1301. <https://doi.org/10.1007/s10518-019-00772-4>
- Pergalani F, Compagnoni M (2008) A procedure for the evaluation of seismic local effects in Lombardia (Italy) for urban planning. In *The 14th World Conference on Earthquake Engineering* (pp. 12–17)
- Pergalani F, Compagnoni M, Colombi A (2011) Development of regional abacuses for level 2 studies finalized to seismic microzonation in Regione Lazio. Proceedings of the 30<sup>th</sup> National Congress of the Gruppo Nazionale di Geofisica della Terra Solida
- Peruzzi G, Albarello D, Baglione M, D’Intinosante V, Fabroni P, Pileggi D (2016) Assessing 1D litho-stratigraphical amplification factor for microzoning studies in Italy. *Bull Earthq Eng* 14:373–389. <https://doi.org/10.1007/s10518-015-9841-z>
- Pilz M, Cotton F (2019) Does the one-dimensional assumption hold for site response analysis? A study of seismic site responses and implication for ground motion assessment using KiK-Net strong-motion data. *Earthq Spectra* 35(2):883–905
- Poggi V, Edwards B, Fäh D (2017) A comparative analysis of site-specific response spectral amplification models. *Physics and Chemistry of the Earth, Parts a/b/c* 98:16–26. <https://doi.org/10.1016/j.pce.2016.09.001>
- Rota M, Zuccolo E, Taverna L, Corigliano M, Lai CG, Penna A (2012) Mesozonation of the Italian territory for the definition of real spectrum-compatible accelerograms. *Bull Earthq Eng* 10:1357–1375. <https://doi.org/10.1007/s10518-012-9369-4>
- Slejko D, Carulli GB, Nicolich R, Rebez A, Zanferrari A, Cavallin A, Doglioni C, Carraro F, Castaldini D, Iliceto V, Semenza E, Zanolla C (1989) Seismotectonics of the eastern Southern-Alps: a review. *Bollettino Di Geofisica Teorica e Applicata* 31:109–136
- Stucchi M, Meletti C, Montaldo V, Crowley H, Calvi GM, Boschi E (2011) Seismic hazard assessment (2003–2009) for the Italian building code. *Bull Seismol Soc Am* 101(4):1885–1911. <https://doi.org/10.1785/0120100130>
- TC4 of ISSMGE (1999) Manual for zonation on seismic geotechnical hazards (revised version). The Japanese Geotechnical Society, pp 219
- Tento A, Martelli L, Marcellini A (2014) Abachi per la valutazione dei fattori di amplificazione per le indagini di microzonazione sismica di secondo livello in Emilia-Romagna. *Atti* 33:289–294 (**in Italian**)
- Tiberi L, Costa G, Suhadolc P (2014) Source parameter estimates for some historical earthquakes in the south-eastern Alps using ground shaking scenarios. *Bollettino di Geofisica Teorica e Applicata*, (55, 3), 641–664 <https://doi.org/10.4430/bgta0121>
- Venturini C, Astori A, Cisotto A (2004) The late Quaternary evolution of central Friuli (NE Italy) as detected through field survey and DEM-derived map analyses. In: Pasquare G, Venturini C, Groppelli G (eds) *Mapping geology in Italy*, Apat-Servizio Geologico d’Italia, IGC Firenze 2004. S.EL.CA, Firenze, pp 95–106
- Working Group ICMS (2008) *Indirizzi e criteri per la microzonazione sismica*. Conferenza delle Regioni e delle Province autonome – Dipartimento della Protezione Civile, Roma, 3 vol. e DVD, (in Italian, available in English at <https://www.centromicrozonazioneismica.it/documents/18/GuidelinesForSeismicMicrozonation.pdf>).
- Working Group ICMS (2011) *Contributi per l’aggiornamento degli Indirizzi e criteri per la microzonazione sismica*. *Ing Sism* anno XXVIII, 2; available online at <https://www.centromicrozonazioneismica.it/it/download/category/17-contributi-per-l-aggiornamento-degli-indirizzi-e-criteri-per-la-microzonazione-sismica> (in Italian)
- Zuccolo E, O’Reilly GJ, Poggi V, Monteiro R (2021) haselREC: an automated open-source ground motion record selection and scaling tool. *Bull Earthq Eng* 19:5747–5767. <https://doi.org/10.1007/s10518-021-01214-w>

**Publisher’s Note** Springer Nature remains neutral with regard to jurisdictional claims in published maps and institutional affiliations.